AIP | Journal of Applied Physics

Second-harmonic generation reveals the oxidation steps in semiconductor processing

M. K. Vanbel, V. K. Valev, B. Vincent, V. V. Afanas'ev, J.-P. Locquet et al.

Citation: J. Appl. Phys. **111**, 064504 (2012); doi: 10.1063/1.3695989
View online: http://dx.doi.org/10.1063/1.3695989
View Table of Contents: http://jap.aip.org/resource/1/JAPIAU/v111/i6
Published by the American Institute of Physics.

Related Articles

Polarization-induced remote interfacial charge scattering in Al2O3/AlGaN/GaN double heterojunction high electron mobility transistors
Appl. Phys. Lett. 100, 132105 (2012)

1-nm-capacitance-equivalent-thickness HfO2/Al2O3/InGaAs metal-oxide-semiconductor structure with low interface trap density and low gate leakage current density
Appl. Phys. Lett. 100, 132906 (2012)

Very low bias stress in n-type organic single-crystal transistors
APL: Org. Electron. Photonics 5, 79 (2012)

Very low bias stress in n-type organic single-crystal transistors
Appl. Phys. Lett. 100, 133301 (2012)

InGaN channel high electron mobility transistor structures grown by metal organic chemical vapor deposition
Appl. Phys. Lett. 100, 121909 (2012)

Additional information on J. Appl. Phys.

Journal Homepage: http://jap.aip.org/
Journal Information: http://jap.aip.org/about/about_the_journal
Top downloads: http://jap.aip.org/features/most_downloaded
Information for Authors: http://jap.aip.org/authors

ADVERTISEMENT

Downloaded 29 Mar 2012 to 134.58.253.57. Redistribution subject to AIP license or copyright; see http://jap.aip.org/about/rights_and_permissions

Second-harmonic generation reveals the oxidation steps in semiconductor processing

M. K. Vanbel,[1] V. K. Valev,[1,2] B. Vincent,[3] V. V. Afanas'ev,[4] J.-P. Locquet,[5] S. Van Elshocht,[3] M. Caymax,[3] and T. Verbiest[1]
[1]*Molecular and Nanomaterials, Department of Chemistry, KU Leuven, 3001 Leuven, Belgium*
[2]*Institute for Nanoscale Physics and Chemistry (INPAC), KU Leuven, 3001 Leuven, Belgium*
[3]*Imec, Kapeldreef 75, 3001 Leuven, Belgium*
[4]*Semiconductor Physics, Department of Physics, KU Leuven, 3001 Leuven, Belgium*
[5]*Solid State Physics and Magnetism, Department of Physics, KU Leuven, 3001 Leuven, Belgium*

(Received 24 August 2011; accepted 20 February 2012; published online 26 March 2012)

Monitoring oxidation steps is an important factor during the fabrication of semiconductor devices, because transistor performance can be greatly affected by defects in the passivation layer. As an example, we discuss the formation of a gate stack in metal oxide semiconductor (MOS) devices using Ge as an alternative channel material. Building an MOS gate stack on Ge requires passivation of the interface between the dielectric (typically a high-k material such as Al_2O_3 or HfO_2, grown by means of atomic layer deposition (ALD)) and the Ge channel. Such passivation can be obtained from a very thin Si layer, epitaxially grown on Ge. The Si surface receives an oxidizing clean (O_3 or wet chemical clean) before the ALD step. In this work, second-harmonic generation (SHG) data are presented for silicon layers with varying thickness, grown with either trisilane (Si_3H_8) or silane (SiH_4) and with various cleaning steps. The trend in second-harmonic response upon azimuthal rotation of the samples was comparable for both silane and trisilane as a Si precursor. Our results show that upon oxidation, the SHG intensity reduces, most likely due to a reduction of the amount of crystalline Si, which is converted to SiO_2. © *2012 American Institute of Physics*. [http://dx.doi.org/10.1063/1.3695989]

I. INTRODUCTION

Transistor performance relies heavily on the condition of the interfaces in the gate stack close to the channel. Therefore it is of utmost importance to understand how the different steps of the manufacturing process influence the electrical passivation of these interfaces.

Especially, for alternative channel materials such as germanium (Ge), this has been shown to be a serious issue.[1] As a potential solution, the use of a thin Si cap layer on top of the Ge is being considered.[2]

In the past few years, research in microelectronics has been driven by scaling down the dimensions of the transistors in integrated circuits, often in agreement with Moore's law.[3–5] This has brought significant challenges for both the manufacturing process and the characterization techniques.[6] As opposed to Si channel devices, where Si forms a natural interface with SiO_2 as a dielectric or interfacial layer, the use of Ge implies additional process steps to grow the channel. Moreover, alternative methods of passivation would need to be employed due to the limitations of GeO_2. Therefore, the use of a thin Si cap layer on top of the Ge is investigated so that the standard passivation schemes known for Si can be considered. However, one of the problems associated with integrating a silicon cap is the unwanted induced segregation of underlying germanium into the silicon cap. This segregation reduces the passivation capacity of the silicon cap. Often, an additional wet cleaning step is needed to reduce the effect of segregation. Clearly, the impact of the Si cap layer thickness and the presence of the additional interfaces between, e.g., Ge and Si, needs to be assessed.[7–9] Although there are many known techniques to analyze surfaces and to measure layer thickness[2] (e.g., spectroscopic ellipsometry (SE), x-ray photoelectron spectroscopy, total x-ray fluorescence, Rutherford backscattering spectroscopy, SE combined with reflectometry), they all have associate limitations with respect to sensitivity, depth resolution, or penetration depth, considering a gate stack consisting of $Ge/Si/SiO_2$ on Si. Furthermore, the latest research in semiconductor industry is focusing on studying specific layers or interfaces embedded in the transistor rather than surface characterization.

A technique such as second-harmonic generation (SHG) is highly suited to investigate buried interfaces.[10–12] SHG is an optical technique with interface sensitivity down to the atomic level.[13] Additionally, the technique has been intensively used in the past to characterize silicon.[14,15] For instance, the optimization with respect to defects at the Si/SiO_2 interface of silicon-on-insulator (SOI) wafers has been investigated using electric field induced second-harmonic (EFISH) generation.[16] Attempts to fully characterize the thickness dependency of SOI wafers have also been made. This research was performed on miscut wafer substrates.[17] The oxidation process itself has been investigated as well by SHG. Heinz *et al.*[18] showed that SHG intensity changes as a function of oxidation time of the top layer of a Si(111) substrate.

Within the electric dipole approximation, SHG is inherently sensitive to non-centrosymmetry, e.g., at interfaces and surfaces. Due to its extreme sensitivity, second-harmonic generation is an ideal candidate for interface probing, allowing the characterization of the passivation of the channel beneath a dielectric, without destroying the sample. Hence,

 © 2012 American Institute of Physics

Downloaded 29 Mar 2012 to 134.58.253.57. Redistribution subject to AIP license or copyright; see http://jap.aip.org/about/rights_and_permissions

the interface can be probed as such or can be characterized upon oxidation.

This paper presents SHG results of silicon cap passivated germanium upon azimuthal rotation of the samples for different thicknesses of silicon cap and for different oxidation steps. Due to the sensitivity of the SHG measurements, the oxidation steps and Si growth are identified and the standard deviation is compared with the error on SE measurements.

II. SAMPLE PREPARATION

The samples were treated differently to obtain a different thickness of the silicon caps and to vary the oxidation conditions. The additional oxidation step to the standard cleaning process is a wet cleaning step prior to an atomic layer deposition (ALD) step, enabling a smoother deposition of dielectric material. The presence of Ge in the Si cap, due to segregation during the Si deposition, can cause the silicon cap to oxidize faster, resulting in a larger oxidation depth.

More specifically, in the initial part of the sample fabrication, Ge was deposited on a (001) cut silicon wafer. Thereafter boron was implanted with a concentration of 10^{16} cm^{-3} at the surface to obtain a p-type (001) Ge semiconductor. Because Ge is a good candidate for use as p-MOS material, the research on germanium is often performed on p-type Ge. An annealing step at 600 °C concluded the preparation of the germanium wafer.

Prior to the Si cap deposition, the surface of the wafer was prepared with a 1 min treatment with a NH_4OH, H_2O_2 and H_2O in a 1:1:5000-mixture, followed by a 5 min de-ionized water rinse. Subsequently, the wafers received a H_2 bake at 650 °C. Silane (SiH_4) or trisilane (Si_3H_8) were used as silicon precursors at deposition temperatures of 500 °C and 350 °C, respectively. The thickness of the Si cap layer, ranging from 2 monolayers (ML) to 6 ML in steps of ~1 ML, was controlled by varying the deposition time (Fig. 1(a)). The thickness of the Si layer was measured with SE on a KLA Tencor F5 spectroscopic ellipsometer. Thicknesses were measured immediately after unloading the samples from the reactor, i.e., without extensive air exposure. The silicon thickness extracted from spectroscopic ellipsometry in nm is transformed into a number of monolayers, assuming 1 ML ≈ 0.13 nm.

For all samples, part of the Si cap was oxidized in ozone for 60 s, forming a native oxide on top. In addition, two samples of 5.4 ML (grown from Si_3H_8) and two samples of 4.2 ML thick (grown from SiH_4), were further oxidized in a 1 ppm ozone-water solution for 60 s followed by a water rinse of 5 min and a cleaning step. This step includes a 120 s 0.5% HF-dip and a 5 min water rinse. After an HF-dip, all oxide is removed from the surface. One sample of the 5.4 and 4.2 ML samples for Si_3H_8 and SiH_4, respectively, is oxidized using ambient oxygen, while the other is oxidized using ozone. The second oxidation step is relevant for reducing the Ge segregation in the silicon layer prior to the ALD process.[2] All samples underwent a Marangoni drying procedure.[19]

Finally, an 8 nm HfO_2 layer is deposited on top of all samples by atomic layer deposition to prevent further oxidation of the wafer. This HfO_2 is formed using $HfCl_4$ as Hf-precursor and water as an oxidizing agent in the ALD process. An overview of the samples with different silicon cap thicknesses is given in Table I.

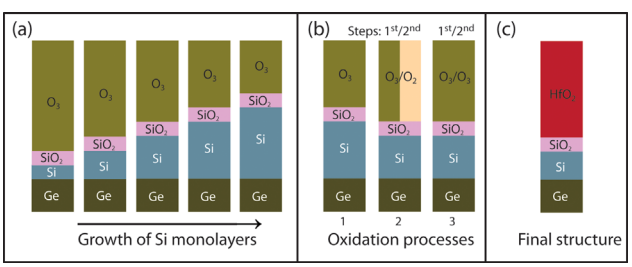

FIG. 1. The growth of the samples and dependency of silicon thickness on the oxidation. (a) Schematic diagram of the monolayer growth of silicon on top of germanium. (b) Schematic diagram of the second oxidation. For samples 2 and 3, the first oxidation is an ozone step, followed by an HF clean, which etches the oxide layer away. Thereafter, an oxidation in ambient O_2 or O_3 is performed. The thickness of the silicon layer decreases because of the etching step. (c) The final structure of the investigated samples.

III. EXPERIMENTAL METHODS AND THEORETICAL DESCRIPTION

The second-harmonic generation experiments are carried out using a Titanium-sapphire (Ti-Al_2O_3) laser at a wavelength of 800 nm with a power output of 130 mW, with a pulse width of approximately 120 femtoseconds and a repetition rate of 82 MHz. The average power density after focusing is approximately 2 kW/cm^2. The beam is initially guided through a half-wave plate and a polarizer to control its polarization. Thereafter the beam passes through a RG 665 filter and is then focused using an achromatic doublet. Subsequently, the beam is incident on the sample at an angle of 45°. The sample is mounted on a rotation stage for azimuthal rotation of the sample. The outgoing beam is collimated with an achromatic doublet and then the beam passes through a BG 36 filter allowing light of 400 nm to pass, while the 800 nm fundamental beam is blocked. When the signal has passed an analyzer, the light is detected by a photomultiplier tube. From different polarizer-analyzer configurations, physical parameters can be extracted upon rotation of the sample. In this experiment, the position of the polarizer and analyzer can be s- or p-polarized, meaning that the electric field is aligned perpendicular or along the plane of incidence, respectively.

For intense electromagnetic fields, such as those generated by a pulsed laser beam, the induced polarization is no longer linearly proportional to the incident electric field $E(\omega)$.[20] Instead, the induced polarization contains higher harmonics of the frequency ω. Among these, the second harmonic polarization $P(2\omega)$ at the double frequency can be written as the sum of dipolar $P^D(2\omega)$ and quadrupolar $P^Q(2\omega)$ polarizations

$$\begin{aligned} P(2\omega) &= P^D(2\omega) + P^Q(2\omega) \\ &= \chi^D : E(\omega)E(\omega) + \chi^Q : E(\omega)\nabla E(\omega), \end{aligned} \quad (1)$$

where ω is the frequency of the light, $E(\omega)$ and $E(\omega)$ are the electric fields of the incident light, and χ^D and χ^Q indicate the dipolar and quadrupolar nonlinear susceptibilities, respectively.

Downloaded 29 Mar 2012 to 134.58.253.57. Redistribution subject to AIP license or copyright; see http://jap.aip.org/about/rights_and_permissions

TABLE I. Summary of the investigated samples

	1.9 ML	2.9 ML	3.7 ML	Sample 1 SiH_4: 4.2 ML	5.6 ML	2.1 ML	2.7 ML	4.1 ML	Sample 1 Si_3H_8: 5.4 ML	6.5 ML	Sample 2 SiH_4	Sample 3 SiH_4	Sample 2 Si_3H_8	Sample 3 Si_3H_8
Preparation of wafers before ALD														
Boron implantation (10^{16} cm^{-3})	x	x	x		x	x	x	x	x	x	x	x	x	x
Annealing step	x	x	x		x	x	x	x	x	x	x	x	x	x
Silicon cap passivation														
10 min H_2 bake at 650 °C, SiH_4 growth at 500 °C		x	x	x	x						x	x		
10 min H_2 bake at 650 °C, Si_3H_8 growth at 350 °C						x	x	x	x	x			x	x
Oxidation step: 1 ppm ozone 60 in.											x	x	x	x
5 min water rinse											x	x	x	x
HF-dip: 120 in. 0.5% HF + 5 min water rinse											x	x	x	x
Oxidation step: 1 ppm ozone 60 in.		x	x	x	x	x	x	x	x	x		x	x	x
Marangoni dry		x	x	x	x	x	x	x	x	x	x	x	x	x
HfO_2 deposition														
HfO_2 ALD (8 nm)	x	x	x	x	x	x	x	x	x	x	x	x	x	x

The susceptibility χ^D is a third rank tensor, which consists of 27 components, but it can be considerably simplified based on the symmetry considerations of the sample. In our case, the Si(001) surface and interfaces are four-fold symmetric in the plane of the sample, hence the susceptibility tensor reduces to[20,21]

$$\chi^D = \begin{pmatrix} 0 & 0 & 0 & 0 & \chi_{xzx} & 0 \\ 0 & 0 & 0 & \chi_{yyz} & 0 & 0 \\ \chi_{zxx} & \chi_{zyy} & \chi_{zzz} & 0 & 0 & 0 \end{pmatrix}, \tag{2}$$

where $\chi_{zxx} = \chi_{zyy}$ and $\chi_{yyz} = \chi_{xzx}$. By changing the polarizer-analyzer configuration, different tensor components can be addressed.

For a (001)-oriented lattice, in the $S_{in} - P_{out}$ polarizer-analyzer configuration, in χ^D a single tensor element is addressed; the dipolar contribution is therefore a constant: P^D_{iso}.

The quadrupolar polarization has the following form:[15,22,24]

$$P^Q(2\omega) = (\delta - \beta - 2\gamma)(\boldsymbol{E}\cdot\nabla)E + \beta E(\nabla\cdot\boldsymbol{E}) + \gamma\nabla(\boldsymbol{E}\cdot\boldsymbol{E}) + \zeta\sum_i \hat{e}_i E_i \nabla_i E_i. \tag{3}$$

For clarity, we omitted the frequency dependence symbol of the fundamental fields. The vectors $\hat{e}_i$ are unit vectors along the crystallographic directions and $\beta, \gamma, \delta, \zeta$ are linear combinations of the χ^Q tensor elements. Considering a single plane-wave excitation, the first term in Eq. (3) is zero, while the second term cancels due to Maxwell's equations.[23] For $S_{in} - P_{out}$, the value of the third term is a constant: P^Q_{iso}. The fourth term is anisotropic and, within the framework of Sipe's theoretical model,[21] in the beam coordinate system $\hat{\mathbf{s}}, \hat{\mathbf{k}}, \hat{\mathbf{z}}$, it can be expressed as

$$\mathbf{P}^Q_{P-out,anis}(2\omega) = in\tilde{\omega}[f_C(f_S\Gamma'^a_{2121} - f_C\Gamma'^a_{2131}) + f_S(f_S\Gamma'^a_{3121} - f_C\Gamma'^a_{3131})]E'_1E'_1, \tag{4}$$

where n is the complex refractive index of the medium, $\tilde{\omega} = \omega/\omega cc, f_C = c/cnn, f_S = \kappa/\kappa(n\tilde{\omega})(n\tilde{\omega})$, κ is the length of a unit vector $\hat{\mathbf{k}}$, while Γ'^a and $\mathbf{E}'$ are both expressions in the $\hat{\mathbf{s}}, \hat{\mathbf{k}}, \hat{\mathbf{z}}$ coordinate system, of on the one hand side, linear combinations of the χ^Q tensor elements and on the other, the fundamental electric field.

Evaluating Eq. (4) leads to

$$\mathbf{P}^Q_{P-out,anis}(2\omega) = in\tilde{\omega}\xi\frac{f_C f_S[1 - \cos4(\phi+\theta)]}{4}E'_1E'_1 = P^Q_{anis}\sin^2 2(\phi+\theta), \tag{5}$$

where P^Q_{anis} regroups all constant terms, ϕ is the angle upon azimuthal rotation, and θ is the phase.

Finally, the intensity of the SHG signal in the $S_{in} - P_{out}$ polarizer-analyzer configuration becomes

$$I_{S_{in}-P_{out}}(2\omega) \propto |P^D_{iso} + P^Q_{iso} + P^Q_{anis}\sin^2 2(\phi+\theta)|^2 \propto |I_0(2\omega)| + |B|\sin^2 2(\phi+\theta) + |A|\sin^4 2(\phi+\theta), \tag{6}$$

Downloaded 29 Mar 2012 to 134.58.253.57. Redistribution subject to AIP license or copyright; see http://jap.aip.org/about/rights_and_permissions

where $I_0(2\omega) = (P^D_{iso} + P^Q_{iso})^2$, while $B = 2(P^D_{iso} + P^Q_{iso})P^Q_{anis}$ and $A = (P^Q_{anis})^2$. The latter term is small with a maximal signal of 10 counts/s, verified by SHG measurements in the $S_{in} - S_{out}$ configuration. In similar systems, the dominating contribution has been reported to have electric-dipole character, originating from the surface.[23] Nevertheless, for Si(001) a large electric-quadrupole response from the bulk has also been reported.[25] Moreover, in some cases it has been shown that contributions from the electric dipole, electric quadrupole, and/or magnetic dipole could be inseparable.[25,26]

Note that we did not include an EFISH term in the total SHG intensity. A possible EFISH contribution is not likely to contribute upon azimuthal rotation. First, the sample was characterized using highly intense laser light, which saturates the photo-induced carriers and defects.[27] This EFISH contribution can be considered to be represented by I_0 in Eq. (6) and is considered constant for all samples. In addition, the inherent EFISH contribution arising from fixed charges at the interface should be constant, due to the 8 nm HfO_2 on top of the total structure, because the total thickness of all oxide layers is approximately constant. The defects, which give rise to an internal electric field, are predominantly present at the SiO_2/HfO_2 interface.[28] The number of charges at the interface are invariant upon growing more Si because of the similarities in the growth procedure. Hence, the voltage drop over the oxide layer is constant.

IV. DISCUSSION AND RESULTS

The SHG experiments were conducted for four different polarizer-analyzer configurations, namely $P_{in} - P_{out}$, $P_{in} - S_{out}$, $S_{in} - P_{out}$, and $S_{in} - S_{out}$; however, only the $S_{in} - P_{out}$ configuration is presented. This configuration is the most informative one, since it only depends on one electric-dipole allowed susceptibility component χ_{zyy} (representative for the surface) in addition to a bulk contribution. Note that we assume that the surface is not reconstructed during deposition of subsequent layers.

The SHG measurements were performed for all samples, grown as specified above. The $S_{in} - P_{out}$ configuration for the samples with a native oxide are presented in Fig. 2, while the samples oxidized with ozone are shown in Fig. 3. The SHG intensity is given as a function of the rotation angle of the sample. From Fig. 2, it can be noticed that the overall intensity of SHG increases with an increasing number of silicon monolayers. The rise in SHG signal is observable for both SiH_4 and Si_3H_8 as Si precursors.

We summarize the possible mechanisms which can induce this increase in SHG intensity. First, due to the strain in the Si interlayer, the tiny increase in material can have a drastic increase in SHG signal.[8] Second, screening of the Ge/Si interface can explain this behavior when the Si/SiO_2 interface is grown. Because the Ge/SiO_2 interface generates less second harmonic than the Si/SiO_2 interface, upon deposition of Si, the "top" interface can screen the "bottom" one. This has been reported previously on similar structures fabricated from other materials.[29,30] Especially, if the tensor components of these interfaces have an opposite sign, the intensity will first decrease and then increase, which can be observed in our experiment. Third, the possibility of contributing quantum well states should not be excluded.[31,32] Due to a change in thickness, the energy band diagram can drastically change, thereby changing the SHG response intensively. Fourth, segregation of Ge in the Si layer is possible and can greatly affect the second-harmonic generation.[33] Those effects can all have an influence on the SHG response.

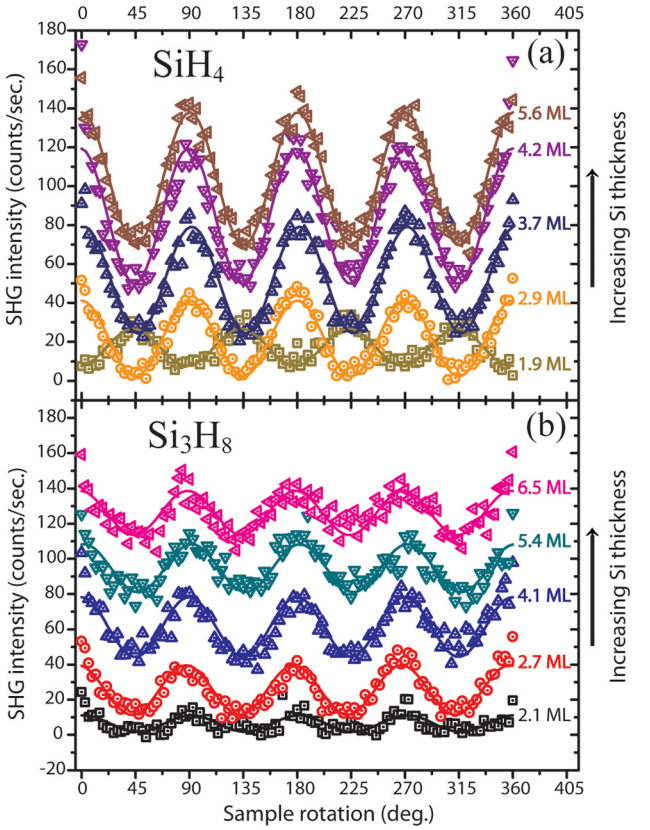

FIG. 2. SHG intensity as a function of sample rotation for various Si thicknesses (in monolayers). The SHG intensity in the S_{in} - P_{out} polarizer-analyzer configuration as a function of sample rotation is shown in (a) and (b) for all samples grown with SiH_4 and Si_3H_8 precursors, respectively. Increasing Si thickness results in an increase in SHG intensity for both precursors. The lines are fittings to Eq. (6).

From Fig. 2, it can be noticed that the phase of the 1.9 ML sample prepared with SiH_4 is shifted 45° compared to the other silicon cap thicknesses. Similar phase shifts have been reported before from Si/oxide[16,27] and Si/metal interfaces[34] and have been attributed to EFISH. In our case, can the phase shift be attributed to EFISH? When measuring the SHG response of semiconducting samples, the high intense laser light can induce charges, which accumulate at the surface or interfaces. These accumulated charges can lead to an internal field and hence EFISH. The samples were subjected to the high intensity laser beam well before starting the experiment. Hence, the EFISH arising from charging of defects is approximately constant when the measurement starts. Consequently, we believe that the phase shift in Fig. 2 is related to the presence of different interfaces during Si growth.[35] More specifically, upon increasing the thickness of Si, first the Ge/SiO_2 interface forms and then the Ge/Si one. Note that the phase shift in Fig. 2(a) is not observed for the

Downloaded 29 Mar 2012 to 134.58.253.57. Redistribution subject to AIP license or copyright; see http://jap.aip.org/about/rights_and_permissions

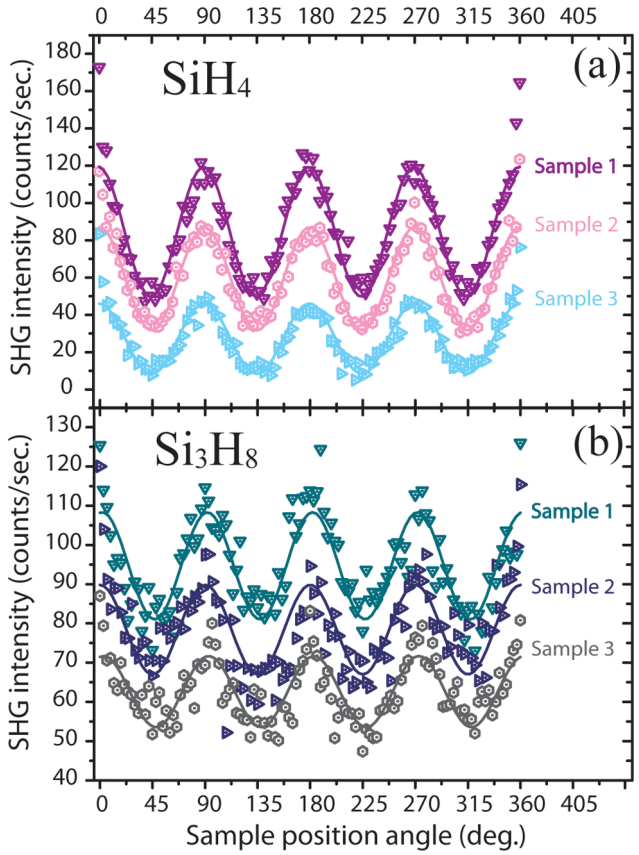

FIG. 3. SHG intensity as a function of oxidation steps. The effect of oxidation on the SHG intensity in the $S_{in} - P_{out}$ polarizer-analyzer configuration is shown in (a) and (b) for SiH_4 and Si_3H_8 precursors, respectively. Sample 1 is a silicon cap passivated Ge wafer with a native oxide. The other samples are oxidized first in ozone and then the oxide layer was etched away. Next, the samples were oxidized in ambient atmosphere (sample 2) or in ozone (sample 3). The lines are fittings to Eq. (6).

layer grown with Si_3H_8, see Fig. 2(b). However, the thickness of the thinnest silicon cap layer of both precursors differs by 0.2 ML. This indicates that between 1.9 and 2.1 ML a silicon onset is introduced, before the layer is fully oxidized. Because the oxidation process is well controlled in length and due to the presence of the HfO_2 layer, the thickness of the SiO_2 layer is thinner than grown as a native oxide in ambient atmosphere.

It should be noted that there is a significant difference in the anisotropic modulation in Fig. 2. This difference can be attributed to the different growth conditions used for the different precursors. The growth temperature for trisilane is 350 °C while for silane the process can only occur at 500 °C. At lower temperatures, the amount of defects introduced in the structure increases. It appears that the enhancement in defect density decreases the anisotropic modulation.[2,33] Due to different temperatures, segregation of Ge into the Si capping layer can be different for both precursors, inducing a difference in anisotropic modulation as well.

In Fig. 3, we show the influence of oxidation on SHG intensity. The first sample was a silicon cap passivated Ge wafer with native oxide without an HF-dip (sample 1). The other samples were oxidized in ozone for 60 s and subsequently the oxide layer is etched away. Next, the samples were exposed to ambient atmosphere (sample 2) or exposed to ozone for 60 s (sample 3). It is clear that the three samples show a drastically different SHG response and that oxidation decreases the overall SHG intensity emanating from the sample. Furthermore, we can clearly distinguish between O_2 and O_3 oxidation. The fact that the SHG intensity decreases upon further oxidation strongly suggests that the SHG signal originates from the silicon. Indeed, the etching step and oxidation step will remove Si and based on the results in Fig. 2, this is accompanied by a strong decrease in SHG intensity. This is in agreement with previous studies of the SHG intensity decrease upon oxidation time.[18] Due to the presence of strain in the Si interlayer, the change in SHG signal can be enhanced.

This thickness dependency can be more clearly seen in Fig. 4, where the isotropic contribution of the total SHG signal, extracted by fitting the total SHG signal using Eq. (6), is plotted as a function of the number of monolayers determined by ellipsometry after each oxidation. The difference in SHG response from the SiH_4 grown silicon layer and Si_3H_8 can be noticed here as well. A very likely explanation for this difference is the variation of Ge segregation. In silane grown Si caps, the segregation is larger than in the trisilane grown structures. Hence, after silicon cap passivation, more Ge is segregated in the silane-formed silicon layer than the trisilane-formed layer. Segregated Ge atoms accumulate at the Si/SiO_2 interface. Upon oxidation, the presence of Ge on the Si surface leads to deeper oxidation of the Si cap. When cleaned with HF, more material is removed and a thinner silicon cap remains. This mechanism could explain the difference in decrease of the silicon cap layer formed by SiH_4 or Si_3H_8.[2] A similar trend is observed when the anisotropic parameter B is plotted as a function of the number of Si monolayers (not shown).

Because second-harmonic generation is not an absolute technique for measuring material thickness, a calibration to

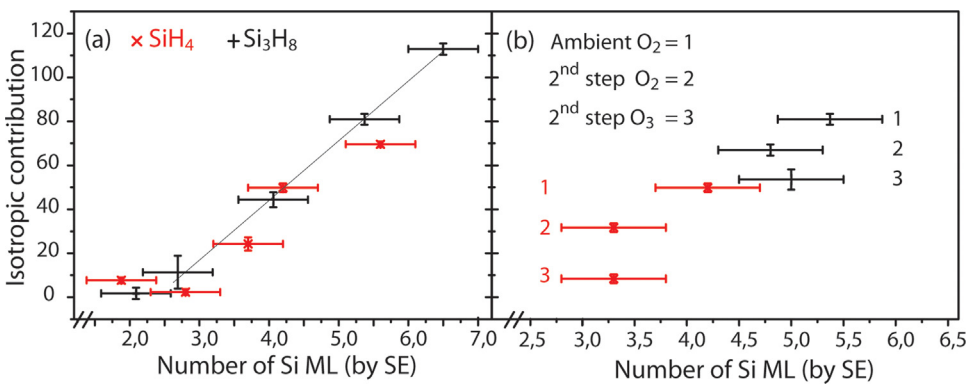

FIG. 4. SHG sensitivity to oxidation steps. The isotropic (surface) contribution for the fitted curves in Figs. 2 and 3 are given as functions of the number of silicon ML in (a) and (b), respectively. The number of monolayers is measured with ellipsometry. The data indicated with an "x" is recorded for SiH_4 as Si precursor, whereas the data indicated with a "+" is for Si_3H_8. For the different oxidized samples, the second oxidation step is specified. The line in (a) is a guide for the eyes.

Downloaded 29 Mar 2012 to 134.58.253.57. Redistribution subject to AIP license or copyright; see http://jap.aip.org/about/rights_and_permissions

complementary measurement techniques would still be necessary for quantitative measurements. In addition, thickness measurements by SHG can only be performed for a well-known process where surface or interface properties are well known. Consequently, second-harmonic generation should be seen as a very accurate technique that requires calibration for quantitative measurements.

It can be clearly observed from Fig. 4 that the SHG intensity decreases, as expected, after the second oxidation step, indicating a decrease in Si thickness. This observation goes beyond the information that can be obtained by ellipsometry measurement alone, due to the standard deviation on the SE measurements. Hence, for silicon cap passivated germanium, the change in silicon thickness as a result of oxidation can be more accurately observed with second-harmonic generation as compared to ellipsometry. Note that the first sample (1.9 ML) grown with silane does not follow the linear trend. This is because all of the silicon oxidized and no silicon interlayer is present in the structure.

V. CONCLUSION

In conclusion, we have shown that second-harmonic generation can be used to characterize buried interfaces with extremely high sensitivity. As a test case, we have found SHG to provide highly accurate relative measurements of the thickness of silicon layers with only a few ML thickness on top of germanium substrates. Furthermore, these results show the subtle differences in oxidizing behavior of the Si layer during oxidizing cleaning steps as a function of the Si precursor used to grow the layer. In the absence of surface roughness or interface defects, we can conclude that SHG can distinguish different oxide treatments during semiconductor growth precisely, in contrast to spectroscopic ellipsometry. This emphasizes the usefulness of SHG as a solid probing technique for buried interfaces. However, thickness measurements by SHG can only be performed for a well-known process where surface or interface properties stay constant. To obtain an absolute measurement of the layer thickness, calibration is needed. In the future, second-harmonic generation can be extended for use in semiconductor growth monitoring and further research on new generations of semiconductor devices.

ACKNOWLEDGMENTS

This work was supported by the Katholieke Universiteit Leuven (GOA and CREA). M.K.V. is grateful for the feedback on the figures and text and trial reading of M. Bloemen, W. Brullot, and S. Vandendriessche. M.K.V. acknowledges the financial support from Imec and the opportunity for collaboration. V.K.V. is grateful for the financial support from the fund for scientific research Flanders (FWO-Vlaanderen).

[1]M. Caymax, G. Eneman, F. Bellenger, C. Merckling, A. Delabie, G. Wang, R. Loo, E. Simoen, J. Mitard, B. De Jaeger, G. Hellings, K. De Meyer, M. Meuris, and M. Heyns, in *Proceedings of the 2009 IEEE International Electron Devices Meeting (IEDM)*, **19**, 1 (2009).
[2]B. Vincent, R. Loo, W. Vandervorst, J. Delmotte, B. Douhard, V. K. Valev, M. Vanbel, T. Verbiest, J. Rip, and B. Brijs, Solid-State Electron. **60**, 116 (2011).
[3]B. Vincent, J. F. Damlencourt, Y. Morand, A. Pouydebasque, C. Le Royer, L. Clavelier, N. Dechoux, P. Rivallin, T. Nguyen, and S. Cristoloveanu, Mater. Sci. Semicond. Process. **11**, 205 (2008).
[4]G. Moore, IEEE J. Solid-State Circuits **20**, 36 (2006).
[5]R. H. Dennard, F. H. Gaensslen, H. Yu, V. L. Rideout, E. Bassous, and A. R. LeBlanc, IEEE J. Solid-State Circuits **9**, 256 (1974).
[6]D. P. Vallett, IEEE Des. Test **14**, 76 (1997).
[7]V. K. Valev, F. E. Leys, M. Caymax, and T. Verbiest, Appl. Phys. Lett. **94**, 061123 (2009).
[8]V. K. Valev, M. K. Vanbel, B. Vincent, V. V. Moshchalkov, M. Caymax, and T. Verbiest, IEEE Electron Device Lett. **32**, 12 (2011).
[9]J. Mitard, C. Shea, B. Dejaeger, A. Pristera, G. Wang, M. Houssa, G. Eneman, G. Hellings, W.-e. Wang, J. C. Lin, F. E. Leys, R. Loo, G. Winderickx, E. Vrancken, A. Stesmans, K. Demeyer, M. Caymax, L. Pantisano, M. Meuris and M. Heyns, Dig. Tech. Pap. - Symp. VLSI Technol. **5**, 82 (2009).
[10]N. H. Tolk, M. L. Alles, R. Pasternak, X. Lu, R. D. Schrimpf, D. M. Fleetwood, R. P. Dolan, and R. W. Standley, Microelectron. Eng. **84**, 2089 (2007).
[11]M. L. Alles, R. Pasternak, X. Lu, N. H. Tolk, R. D. Schrimpf, D. M. Fleetwood, R. P. Dolan, and R. W. Standley, IEEE Trans. Semicond. Manuf. **20**, 107 (2007).
[12]J. Litwin, J. Sipe, and H. M. van Driel, Phys. Rev. B **31**, 5543 (1985).
[13]V. Valev, A. Kirilyuk, F. Dalla Longa, J. Kohlhepp, B. Koopmans, and Th. Rasing, Phys. Rev. B **75**, 012401 (2007).
[14]G. Lüpke, Surf. Sci. Rep. **35**, 75 (1999).
[15]J. McGilp, Prog. Surf. Sci. **49**, 1 (1995).
[16]B. Jun, Y. V. White, R. D. Schrimpf, D. M. Fleetwood, F. Brunier, N. Bresson, S. Cristoloveanu, and N. H. Tolk, Appl. Phys. Lett. **85**, 3095 (2004).
[17]W. S. Kolthammer, D. Barnard, N. Carlson, A. D. Edens, N. A. Miller, and P. N. Saeta, Phys. Rev. B **72**, 045446 (2005).
[18]T. F. Heinz, M. M. T. Loy, and W. A. Thompson, J. Vac. Sci. Technol. B **3**, 1467 (1985).
[19]A. F. M. Leenaars, J. A. M. Huethorst, and J. J. Van Oekel, Langmuir **6**, 1701 (1990).
[20]T. Verbiest, K. Clays, and V. Rodriguez, *Second-order Nonlinear Optical Characterization Techniques* (CRC Press, New York, 2009).
[21]J. Sipe, D. Moss, and H. M. van Driel, Phys. Rev. B **35**, 1129 (1987).
[22]N. Bloembergen, R. K. Chang, S. S. Jha, and C. H. Lee, Phys. Rev. **174**, 813 (1968).
[23]P. Guyot-Sionnest, W. Chen, and Y. R. Shen, Phys. Rev. B **33**, 8254 (1986).
[24]M. Falasconi, L. C. Andreani, A. M. Malvezzi, M. Patrini, and V. Mulloni, Surf. Sci. **481**, 105 (2001).
[25]D. J. Bottomley, G. Lupke, C. Meyer, and Y. Makita, Opt. Lett. **5**, 453 (1995).
[26]C. W. van Hasselt, M. A. Verheijen, and Th. Rasing, Phys. Rev. B **42**, 9263 (1990).
[27]T. Scheidt, E. G. Rohwer, P. Neethling, H. M. von Bergmann, and H. Stafast, J. Appl. Phys. **104**, 083712 (2008).
[28]V. S. Kaushik, B. J. O'sullivan, G. Pouroit, N. Van Hoornick, A. Delabie, S. Van Elshocht, W. Deweerd, T. Schram, L. Pantisano, E. Rohr, L.-A. Ragnarsson, S. De Gendt, and M. Heyns, IEEE Trans. Electron Devices **53**, 2627 (2006).
[29]Q. Y. Jin, H. Regensburger, R. Vollmer, and J. Kirschner, Phys. Rev. Lett. **80**, 4056 (1998).
[30]J. Hamrle, L. Polerecký, and J. Ferré, Phys. Rev. B **68**, 144401 (2003).
[31]H. A. Wierenga, M. W. J. Prins, and Th. Rasing, Physica B **204**, 281 (1995).
[32]Th. B. Kristensen, K. Pedersen, and Th. G. Pedersen, Phys. Status Solidi A **175**, 195 (1999).
[33]B. Vincent, R. Loo, W. Vandervorst, G. Brammertz, and M. Caymax, J. Cryst. Growth **312**, 2671 (2010).
[34]J. I. Dadap, X. F. Hu, M. H. Anderson, M. C. Downer, J. K. Lowell, and O. A. Aktsipetrov, Phys. Rev. B **53**, 7607 (1996).
[35]H. Hirayama, T. Komizo, T. Kawata, and K. Takayanagi, Appl. Surf. Sci. **190**, 180 (2002).

Downloaded 29 Mar 2012 to 134.58.253.57. Redistribution subject to AIP license or copyright; see http://jap.aip.org/about/rights_and_permissions